Strong Photonic Localizations Generated in Single-Optical-Waveguide Ring
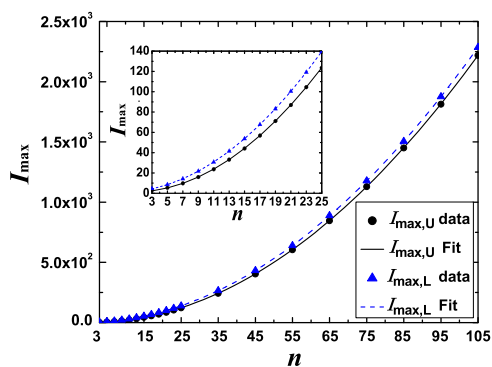
Nana Wang
Xiangbo Yang
Xiaohui Xu
Yuehua Huang
Peichao Cao
Dongmei Deng
Chengyi Timon Liu
Xubo Hu

IEEE

Strong Photonic Localizations Generated in Single-Optical-Waveguide Ring

Nana Wang,[1] **Xiangbo Yang,**[1,2,3] **Xiaohui Xu,**[1] **Yuehua Huang,**[1]
Peichao Cao,[1] **Dongmei Deng,**[2] **Chengyi Timon Liu,**[3] **and Xubo Hu**[2,4]

[1]MOE Key Laboratory of Laser Life Science and Institute of Laser Life Science, College of Biophotonics, South China Normal University, Guangzhou 510631, China
[2]Guangdong Provincial Key Laboratory of Nanophotonic Functional Materials and Devices, South China Normal University, Guangzhou 510631, China
[3]School of Physical Education and Sports Science, South China Normal University, Guangzhou 510006, China
[4]College of Electronic Engineering, South China Agricultural University, Guangzhou 510642, China

Abstract: In this paper, an extreme simple single-optical-waveguide ring (SOWR) is designed to generate strong photonic localizations by considering the similarities between electrons in electronic mesoscopic networks and photons in optical waveguide networks (OWNs). This interesting structure is designed based on the single-electronic-mesoscopic ring that can produce huge electronic persistent currents. We obtain the fitting formulas of the intensity, site number, and site positions for the maximal photonic localization in a SOWR. These interesting SOWRs may provide attractive applications like multichannel high-efficiency energy storages, high power super luminescent light emitting diodes, optical switches, and other correlative all-optical devices. Moreover, the approach of referencing single-electronic-mesoscopic ring to design SOWR may offer a new way to devise optical structures being capable of producing strong photonic localizations and may also deepen people's knowledge on the correlation between OWN and the electronic mesoscopic network.

Index Terms: Localization, single-optical-waveguide ring (SOWR), waveguide.

1. Introduction

In 1987, Yablonovitch [1] and John [2] found that when propagated in a dielectric structure with periodic arrangement, the transmission of electromagnetic (EM) waves is inhibited in certain frequency areas, which are known as photonic band gaps (PBGs). So far, PBG materials still have been one of the foci in physics, optics, material science, and so on [3]–[11]. The network systems made of 1-D waveguides, a kind of PBG structure, that have been widely studied and attracted great concern [12]–[20]. Compared with usual PBG materials, optical waveguide networks (OWNs) possess many advantages. They are experimentally easily realizable due to their structural

flexibility. Additionally, the phase, amplitude and wave function can be measured anywhere. It is well known that PBG and photonic localization are two main features of PBG materials. Generally, for the optical devices based on photonic localization, the stronger the photonic localizations are, the better the functions will be. It is of great importance for designs such as multi-channel high efficiency energy storages [21], [22], optical switches [23], high power super luminescent light emitting diodes [24], [25], etc. Consequently, how to design OWNs that are capable of producing strong photonic localizations has received extensive attention in optics, physics, material science, and other related fields.

In 1998, Zhang *et al.* [13] studied photonic localizations in a three-dimensional OWN. In 2005, Sengupta *et al.* [26] investigated the intensity distribution of photonic localization in 1D Fibonacci OWN. However, the intensities of photonic localization generated by aforementioned OWNs [13], [26] are relatively lower. In 2014, Tang [27] designed symmetric two-segment-connected triangular defect waveguide networks, and found that the maximal intensity of photonic localization increases as an exponential function with the increment of the number of unit cells, and increases as an inverse-squared function to the increment of the breaking degree. Moreover, in 2015, Cheng *et al.* [10] investigated Symmetric Fibonacci superlattices and found that as the generation order increases, the maximum value of squared electric field increases exponentially. Although the aforementioned OWNs [10], [27] can generate very strong photonic localization, the structures of them are all extraordinary complex, because in an OWN each node requires a matching transducer connector. The more the nodes there exist, the more the transducer connectors are needed. It means that the OWN structure will be more complex and more difficult to be achieved experimentally, and then the higher cost will be accompanied. It is challenging but worthwhile to devise an OWN that not only creates stronger photonic localizations but possesses simpler structure than previous OWNs as well. In order to solve this problem, in this paper we present a single-optical-waveguide ring (SOWR) in referencing to the single-electronic-mesoscopic ring able to produce a huge electronic persistent current [28], which exhibits very strong photonic localizations and possesses simplest structure.

Different from macroscopic systems, the electronic transportation in mesoscopic systems exhibits many fantastic properties [29]. For example, a persistent current can be reproduced from a metal ring and it flows through the resistive circuit without decaying. Strong persistent currents can be tested easily by experiments and possess important applications in microcircuits, so people have paid much attention to how to obtain strong persistent current. Our recent research [28] shows that in the absence of external magnetic field, stub, and impurity, a single-electronic-mesoscopic ring can create a huge electronic persistent current whose maximal amplitude is dependent on loop length quantum number n linearly. To the best of our knowledge, a necessary (but not sufficient) condition for an electronic mesoscopic structure to produce huge electronic persistent current is the existence of strong electronic localization. As a consequence, if an electronic mesoscopic structure is able to generate giant electronic persistent current, there definitely exist strong electronic localizations. It has been recognized that both electrons propagating in an electronic mesoscopic structure [30] and photons transmitting in an OWN [15] all exhibit undulatory property and even share same wave functions. Thus, we anticipate that the OWN with the same structure of electronic mesoscopic one will also generate strong photonic localizations. Therefore, we design a SOWR based on the single-electronic-mesoscopic ring [28] able to produce huge electronic persistent currents and find that the SOWR can indeed reproduce very strong photonic localizations. Compared with other reported OWNs being capable of producing strong photonic localizations, our designed SOWR can not only generate large photonic localizations but possesses the simplest structure as well. Moreover, this approach of referencing the single-electronic-mesoscopic ring to design the SOWR may offer a new way for devising optical structures being capable of generating strong photonic localizations, and may also deepen people's knowledge on the correlation between OWN and electronic mesoscopic network.

This paper is organized as follows. In Section II, we introduce the structure of our designed SOWR, generalized eigenfunction method, and the methods for calculating intensity of photonic localization and photonic frequency of maximal photonic localization. The numerical results and
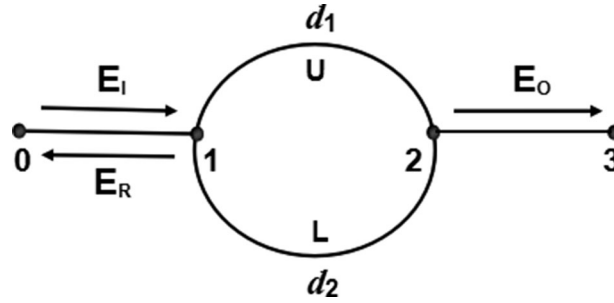
Fig. 1. Schematic diagram of the 1-D SOWR with one entrance and one exit, where U and L represent the upper and lower arms with the lengths of d_1 and d_2, respectively. E_I, E_R, and E_O are the input, reflective, and output EM waves, respectively.

discussions of the maximal photonic localizations in SOWR are presented from three aspects in Section III. Finally, a conclusion is given in Section IV.

2. Model and methods

A. Model

Our recent research [28] shows that the single-electronic-mesoscopic ring can produce huge electronic persistent currents. In this paper, we study the maximal photonic localizations generated by SOWR which is designed by referencing the structure of the single-electronic-mesoscopic ring. Therefore, the structure of SOWR is as the same as that of our previous designed single-electronic-mesoscopic ring [28]. However, the materials of them are different. The latter is made up of ideal 1-D metallic wires, while the former is made up of 1-D vacuum optical waveguide segments. The structure of SOWR is shown in Fig. 1.

In Fig. 1, the SOWR contains an entrance, an exit, an upper arm, and a lower arm, where both the lengths of the optical waveguide segments connected with the entrance and exit are all d_1, those of the upper and lower arms are, respectively, d_1 and d_2, and the ring circumference is D. Our results for the single-electronic-mesoscopic ring [28] show that the maximal persistent current increases linearly with the increment of the loop length quantum number n, which is defined as follows. After simplifying the ratio of the length of upper arm to the ring circumference, $d_1 : D$, to be that of relative prime numbers, i.e., $d_1 : D = m : n$, we call this pair of positive integers m and n upper arm quantum number and loop length one, respectively. First, m is a positive integer, so when n is odd, it must be greater than or equal to 3. Second, our studies show that when n is even and smaller than 8, intensities of maximal photonic localizations generated in SOWR are all very small and we do not care about these cases. Therefore, when n is even, it must be greater than or equal to 8. Taking into account these two factors, we divide SOWRs into three types according to n: SOWRs with odd n, those with even n being divided exactly by 4, and those with even n being divided inexactly by 4.: The loop length quantum number n for these three types of SOWRs can be expressed as follows

$$n = \begin{cases} 2j+1 & \text{(Type I)} \\ 4j & \text{(Type II)} \\ 2(2j+1) & \text{(Type III)} \end{cases} \tag{1}$$

where, for Type I $j \geq 1$, and for Types II and III, $j \geq 2$. On ther other hand, for micro and nano scale structure, when the length ratio of the upper and lower arms is more approaching 1, the structure will be relatively easier to fabricate. Therefore, for the above three types of SOWRs, we only care about those which ratio of m to n tends to be 1/2, i.e., the ratio of $m : n$ for these three types of

SOWRs can be expressed as follows:

$$m : n = \begin{cases} j : (2j + 1) & \text{(Type I)} \\ (2j - 1) : 4j & \text{(Type II)} \\ (2j - 1) : [2(2j + 1)] & \text{(Type III)}. \end{cases} \tag{2}$$

B. Intensity of Photonic Localization

The SOWR we study is formed by 1-D waveguide segments where only monomode propagation of EM waves needs to be considered. The EM wave function with angular frequency ω in any segment between nodes i and j can be regarded as a linear combination of two opposite traveling plane waves

$$\psi_{ij}(x) = A_{ij}e^{\iota k_o x} + B_{ij}e^{-\iota k_o x}, \tag{3}$$

where $k_o = \omega/c$, and c is the speed of the EM wave in the vacuum. The EM wave function between nodes i and j can also be expressed as follows [15]:

$$\psi_{ij}(x) = \frac{\sin k_o (l_{ij} - x)}{\sin k_o l_{ij}} \psi_i + \frac{\sin k_o x}{\sin k_o l_{ij}} \psi_j \tag{4}$$

where ψ_i and ψ_j are the wave functions at nodes i and j, respectively, and l_{ij} is the length of the segment between nodes i and j. In this paper we define the intensity of photonic localization anywhere as

$$I(x) = \left| \psi_{ij}(x) \right|^2. \tag{5}$$

C. Generalized Eigenfunction Method

By means of the energy flux conservation one can deduce that the EM wave function at each node satisfies the following network equation [14], [15], [31]

$$-\psi_i \sum_j \cot k_o l_{ij} + \sum_j \psi_j \csc k_o l_{ij} = 0. \tag{6}$$

At the entrance and exit of SOWR, by use of (3), one can obtain the normalized wave functions as follows

$$\begin{aligned} \psi_0 &= 1 + r \\ \psi_1 &= e^{\iota k_o d_1} + re^{-\iota k_o d_1} \\ \psi_2 &= t \\ \psi_3 &= te^{\iota k_o d_1} \end{aligned} \tag{7}$$

where r and t are reflection and transmission coefficients, respectively. By means of (6), one can deduce the relationship among the wave functions of the two nodes of SOWR. Combining it with (7), one can calculate the transmission coefficient t, and then obtain the transmissivity T by the formula $T = |t|^2$. In this paper, the generalized eigenfunction method [32] is used for computing t, where the coefficients r and t are all treated as generalized wave functions. After changing the united equation set into a 4 order matrix, the problem of solving wave function has been changed into that of calculating eigenvalues by software. One can calculate transmission coefficient t and the wave functions at nodes 1 and 2, i.e., ψ_1 and ψ_2.

By use of (4), and (5), one can calculate the intensity of photonic localization anywhere within a SOWR. However, the photonic frequency f_o in the formula is still unknown, we will introduce the method of computing f_o in Section II-D.

D. Photonic Frequency of Maximal Photonic Localization

In this paper, we mainly study the properties of the maximal photonic localizations in the SOWR. The photonic frequencies are calculated indirectly by the electronic persistent current in the single-electronic-mesoscopic ring.

It is well known that if an electronic mesoscopic ring is able to generate a giant electronic persistent current, there definitely exists strong electron localizations. Based on previous works [15], [30], one knows that both electrons propagating in an electronic mesoscopic structure [30] and photons transmitting in an OWN [15] all exhibit same undulatory property and even their wave functions are all the same. Therefore, the OWN with the structure as the same as that of an electronic mesoscopic ring can generate strong photonic localizations. On this condition, the wave number of electrons, k_e, for the strongest electronic localizations is equal to that of photons, k_o, for the maximal photonic localizations. According to our recent work [28], one knows that only when the electrons with the specific wave number of k_e propagate in the single-electronic-mesoscopic ring, can the strongest electronic localizations be produced, where k_e can be deduced by the phase(s) of the narrowest valley(s) in the electronic persistent current spectrum. It can be deduced that $k_e = \theta_e/D$, $k_o = 2\pi f_o/c$. Then, for a SOWR with the ratio of upper arm to loop length, $m : n$, and the ring circumference of D, the photonic frequency for the maximal photonic localization can be expressed as follows:

$$f_o = \frac{\theta_e c}{2\pi D}. \tag{8}$$

Consequently, in this paper, the computational process of the maximal photonic localization in a SOWR are as follows: First, calculate the electronic persistent current spectrum. Second, determine the phase θ_e of the maximal electronic localization by electronic persistent current spectrum. Third, obtain the photonic frequency for the maximal photonic localization by means of (8). Finally, investigate the maximal photonic localization in the SOWR by use of (5).

Now, we introduce the calculation method of the electronic persistent current in single-electronic-mesoscopic ring. Based on previous work [15], [28], [30], one knows that the single-electronic-mesoscopic ring is composed of circuits of 1-D ideal metallic wires; then, only monomode propagation of electronic wave needs to be considered, and the wave function in each circuit can also be regarded as a linear combination of two opposite traveling plane waves whose wave function form is (3). For single-electronic-mesoscopic ring the wave functions of the upper and lower arms can be written as follows:

$$\psi_U(x) = A_U e^{\iota k_e x} + B_U e^{-\iota k_e x}$$

$$\psi_L(x) = A_L e^{\iota k_e x} + B_L e^{-\iota k_e x} \tag{9}$$

where

$$\begin{pmatrix} A_U & B_U \\ A_L & B_L \end{pmatrix} = \begin{pmatrix} \dfrac{\psi_2 - \psi_1 e^{-\iota k_e d_1}}{e^{\iota k_e d_1} - e^{-\iota k_e d_1}} & \dfrac{\psi_1 e^{\iota k_e d_1} - \psi_2}{e^{\iota k_e d_1} - e^{-\iota k_e d_1}} \\ \dfrac{\psi_2 - \psi_1 e^{-\iota k_e d_2}}{e^{\iota k_e d_2} - e^{-\iota k_e d_2}} & \dfrac{\psi_1 e^{\iota k_e d_2} - \psi_2}{e^{\iota k_e d_2} - e^{-\iota k_e d_2}} \end{pmatrix}. \tag{10}$$

From (9), one can get the probability current [33] in the upper and lower arms as follows:

$$J_U = |A_U|^2 - |B_U|^2$$

$$J_L = |A_L|^2 - |B_L|^2. \tag{11}$$

Then, the electronic persistent current [28], [33] in single-electronic-mesoscopic ring can be obtained as follows:

$$J_P = \frac{T - |J_U| - |J_L|}{2}. \tag{12}$$

As an example, we make use of one of Xiao's results [28] for the single-electronic-mesoscopic ring with $m : n = 4 : 9$ to show the computation process of determining the photonic frequency
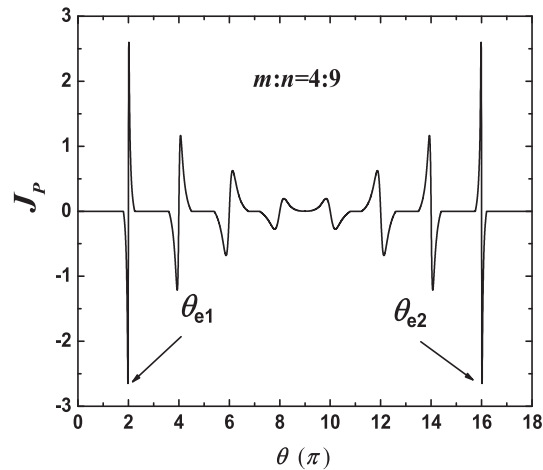
Fig. 2. Electronic persistent current spectra of the single-electronic-mesoscopic ring with $m : n = 4 : 9$, where θ_{e1} and θ_{e2} represent the two phases of the maximal electronic persistent current, respectively [28].

for the maximal photonic localization. First, by means of (12), one can calculate the spectrum of electronic persistent current in the single-electronic-mesoscopic ring. The results are shown in Fig. 2 [28]. Second, determine the phase θ_e of the maximal electronic localization by Fig. 2. From Fig. 2, one can see that the phases of the two narrowest valleys are $\theta_{e1} = 1.9824\pi$ and $\theta_{e2} = 16.0176\pi$, respectively. Third, by means of (8) one can obtain that the two photonic frequencies for the maximal photonic localization are, respectively, $f_{o1} = 0.991188c/D$ and $f_{o2} = 8.008812c/D$. Finally, by use of (5), one can investigate the maximal photonic localization in the SOWR. In Section III, we use this method to study the properties of the maximal photonic localizations in SOWRs.

3. Numerical results and discussions

In this section, we study in detail the intensity I_{max}, the number N, and the positions x_{max} for the sites of the maximum photonic localization in the three aforementioned types of SOWRs.

A. Intensity of Maximal Photonic Localization I max

From numerical results we find that in a SOWR photons with some special frequencies can produce giant photonic localizations. The intensity of the maximal photonic localization I_{max} is closely related to the loop lenght quantum number n and the fitting formula is

$$I_{max,\nu}(n) = C_{1\nu}n^2 + C_{2\nu}n + C_{3\nu} \qquad (\nu = U, L) \qquad (13)$$

where U and L represent the upper and lower arms, respectively. The values of coefficients $C_{i\nu}(i = 1, 2, 3; \nu = U, L)$ are shown in Table 1.

i) From (13), one can see that I_{max} increases as a quadratic function with the increment of n. Table 1 shows that $C_{1\nu} > 0$, it means the shape of the quadratic function is an opening upward parabolic profile. ii) Based on mathematic knowledge one knows that the abscissa of the valley of the parabola is $n_{min,\nu} = -C_{2\nu}/2C_{1\nu}$. From Table 1, one can see that $C_{1\nu} > 0$ and $C_{2L} > 0$, so for the lower arm, $n_{min,L} < 0$. On the other hand, from Table 1 one can also see that $C_{1\nu} > 0$ and $-1.8 < C_{2U}/C_{1U} < 0$, and then for the upper arm, $0 < n_{min,U} < 0.9$. Additionally, (1) shows that n_{min} in our studied SOWR is 3; therefore, for upper and lower arms, $n > n_{min,\nu}$. Based on i) and ii), one can deduce that in a SOWR, I_{max} increases monotonously as a quadratic function with the increment of n. From Table 1, one knows that $C_{2U} < 0$ and $C_{2L} > 0$; then, it can be deduced that $I_{max,U} < I_{max,L}$.

TABLE 1

Values of coefficients in (13) for three types of SOWR

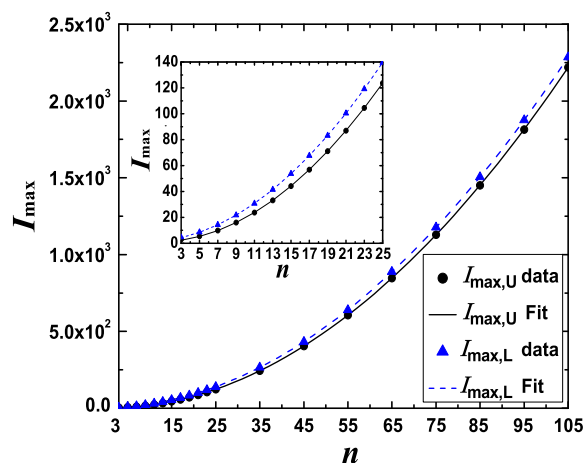| Type	C_{1U}	C_{2U}	C_{3U}	C_{1L}	C_{2L}	C_{3L}
I	0.2027	−0.1615	1.0150	0.2027	0.4750	1.0240
II	0.0507	−0.0817	1.1350	0.0507	0.2370	1.1061
III	0.0507	−0.0807	1.1963	0.0507	0.2369	1.2690

Fig. 3. I_{max} versus n in the upper and lower arms of type I SOWRs. The black spots (blue triangles) represent the numerical results of $I_{max,U}$ ($I_{max,L}$). The black solid (blue dash) line denotes the results of fitting formula of $I_{max,U}$ ($I_{max,L}$) in (13).

These results can be explained as follows. It is known that in an electronic mesoscopic network, electrons can produce huge electronic persistent current because of coulomb actions among electrons, quantum resonant effect, and strong electronic localizations. In the electronic mesoscopic ring [28], a giant electronic persistent current is generated and it means strong electronic localizations are created there. Now, it is also known that electrons propagating in an electronic mesoscopic structure [30] and photons transmitting in an OWN [15] not only all exhibit undulatory property but possess identical wave functions as well. Therefore, photons in a SOWR can certainly reproduce very strong localizations just as electrons in an electronic-mesoscopic-ring do. Due to the quantum resonance effect of loop length, the larger the n is, the more the resonant states are produced, then the more the number of photonic state will be, and consequently, the larger the intensity of maximal photonic localization will be produced in a SOWR. This is the physical mechanism that I_{max} increases monotonously with the increment of n in a SOWR. According to (2), one knows that the upper arm quantum number is smaller than the lower arm quantum number in our designed SOWR, therefore, the intensity of maximal photonic localizations generated in upper arm is smaller than that created in lower arm, i.e., $I_{max,U} < I_{max,L}$.

As an example, by use of type I SOWRs, we verify the fitting formula in (13) and the results in Table 1. First, from (1) and (2), one can obtain that for type I SOWRs, $m : n = j : (2j + 1)$, where $j \geq 1$. Then, by means of (5) one can calculate the numerical results of I_{max} in the upper and lower arms. We plot them as black spots and blue triangles in Fig. 3, respectively. Furthermore, making use of (13) and Table 1, we draw the curves of $I_{max,U}$ and $I_{max,L}$ decided on the fitting formula as the

TABLE 2

Site number of the maximal photonic localizations for three types of SOWRs

Type	$N_{U-f_{n1}}$	$N_{L-f_{n1}}$	$N_{U-f_{n2}}$	$N_{L-f_{n2}}$
I	1	1	$n-2$	n
II	1	1	$n/2-2$	$n/2$
III	$(n-6)/4$	$(n+2)/4$	$(n-2)/4$	$(n+6)/4$

black solid line and blue dash line in Fig. 3, respectively. From Fig. 3, one can see that all spots are on the curves, which means that the numerical calculations are accordant with the fitting formula.

B. Site Number of Maximal Photonic Localizations N

From numerical results, we find that when EM waves propagate in a SOWR with loop length quantum number n, there exist two photonic frequencies for the maximal photonic localization, we call them f_{n1} and f_{n2} and $f_{n1} < f_{n2}$. Furthermore, for the photonic frequency f_{n1} (f_{n2}) we call the site number of the maximal photonic localization in the upper and lower arms $N_{U-f_{n1}}$ and $N_{L-f_{n1}}$ ($N_{U-f_{n2}}$ and $N_{L-f_{n2}}$), respectively. The results of the site number for the maximal photonic localizations are listed in Table 2. The rules are as follows. i) In type I SOWRs, for the EM waves with frequency f_{n1} there only exists one site of maximal photonic localization in both upper and lower arms. For the EM waves with frequency f_{n2} there exist more than one sites of maximal photonic localizations in both upper and lower arms. The site number increases linearly with the increment of n and the growth rate is 1. ii) In type II SOWRs, for the EM waves with frequency f_{n1}, there only exists one site of maximal photonic localization in both upper and lower arms. For the EM waves with frequency f_{n2} there exist more than one sites of maximal photonic localizations in both upper and lower arms. The site number increases linearly with the increment of n and the growth rate is 1/2. iii) In type III SOWRs, for the EM waves with frequencies f_{n1} and f_{n2} there exist more than one sites of maximal photonic localizations in both upper and lower arms. The site number increases linearly with the increment of n and the growth rate is 1/4. From subSection III-A, one knows that I_{max} increases as a quadratic function with the increment of n, so the SOWRs with single (multi) sites of maximal photonic localizations possess potential applications of single- (multi-) channel high efficiency energy storages. Obviously, from (13) and Tables I and II one can see that in type I SOWRs, I_{max} and site number of the maximal photonic localization all grow fastest with the increment of n. For the three types of SOWRs, type I SOWRs are the potential single- (multi-) channel energy storages with highest efficiency.

As examples of types I, II, and III SOWRs, we use the SOWRs with $m:n = 4:9$, $7:16$, and $5:14$ to verify the results in Table 2. By means of (5) one can calculate the intensities of photonic localization. We plot the results of the aforementioned three SOWRs in Fig 4, where the blue dash (red solid) lines represent the results of the EM waves with frequency f_{n1} (f_{n2}). Figs. 4(a) and 4(d) are the intensity maps of EM waves propagating in the upper and lower arms of the SOWR with $m:n = 4:9$, which belongs to the type I SOWRs and the blue dash and red solid lines represent the results of the EM waves with frequencies $f_{91} = 0.991188c/D$ and $f_{92} = 8.008812c/D$, respectively. In Figs. 4(a) and (d), there only exists 1 peak in blue dash lines for the upper and lower arms, which corresponds to the EM waves with the frequency of f_{91}, while for the EM waves with the frequency of f_{92}, there exist 7 and 9 peaks in red solid lines for the upper and lower arms, respectively. From Table 2 one can see that for type I SOWRs, the site numbers of the maximal photonic localization in both upper and lower arms are all only one for the EM waves with frequency f_{91}. For the EM waves
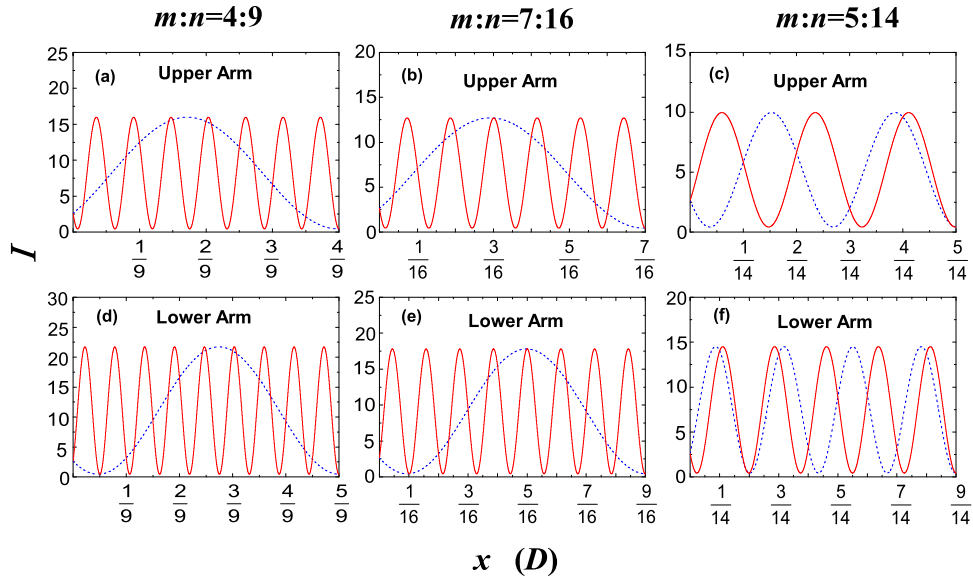
Fig. 4. Intensity maps of EM waves propagating in the SOWRs with $m:n = 4:9$, $7:16$ and $5:14$, respectively. The blue dash (red solid) lines represent the results for the EM waves with frequencies f_{n1} (f_{n2}).

TABLE 3

Values of coefficients in (14) for EM waves with frequency f_{n1} propagating in types I and II SOWRs

Type	C_{4U}	C_{5U}	C_{6U}	C_{4L}	C_{5L}	C_{6L}
I	−0.70	−1.13	0.25	0.49	−1.00	0.25
II	−1.55	−1.13	0.25	1.00	−1.00	0.25

with frequency of f_{92}, the site numbers of the maximal photonic localization in upper and lower arms are, respectively, $n-2$ and n. Obviously, the numerical results are accordant with Table 2. Similarly, one can also see that the results of the SOWRs with $m:n = 7:16$ and $5:14$ accord with Table 2, as well.

C. Site Positions of Maximal Photonic Localizations x_{max}

In this subsection, we investigate the site positions of maximal photonic localizations of three types of SOWRs. We define the distance from the qth site of maximal photonic localization to node 1 as $x_{max,\nu q}$ ($\nu = $ U, L). The rules of site positions are as follows.

i) From Section III-B one knows that for the EM waves with frequency f_{n1} in types I and II SOWRs, there only exists 1 site of maximal photonic localization both in upper and lower arms. We obtain the following fitting formula of $x_{max,\nu 1}$:

$$x_{max,\nu 1} = C_{4\nu}n^{C_{5\nu}} + C_{6\nu} \tag{14}$$

and the values of coefficient $C_{i\nu}(i = 4, 5, 6; \nu = $ U, L) are shown in Table 3.

From (14) and Table 3, one can see that for the EM waves of frequency f_{n1}, $x_{max,U1}$ ($x_{max,L1}$) is the power function of n in both types I and II SOWRs. For the upper arm, $C_{4U} < 0$, $C_{5U} < 0$,
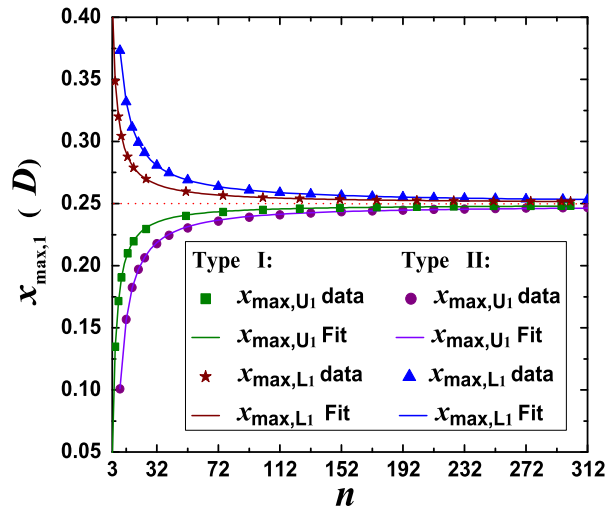
Fig. 5. $x_{\max,\nu 1}$ versus n in the upper and lower arms of type I and II SOWRs for the EM waves with frequency f_{n1}.

and $C_{6U} = 0.25$, it means that (14) is a monotonous increasing power function, whose asymptote is $x_{\max,U1} = 0.25 = 1/4$. Therefore, in the upper arm the distance from the maximal photonic localization site to node 1 increases monotonously with the increment of n, it tends to the midpoint of the upper arm from left to right gradually. For the lower arm, $C_{4L} > 0$, $C_{5L} < 0$, and $C_{6L} = 0.25$, it means that (14) is a monotonous decreasing power function, whose asymptote is $x_{\max,L1} = 0.25 = 1/4$. Therefore, in the lower arm the distance from the maximal photonic localization site to node 1 decreases monotonously with the increment of n, it tends to the midpoint of the lower arm from right to left gradually. The determination of the site positions of the maximal photonic localization in a SOWR helps to determine the connection positions of energy storage device. Therefore, the larger the loop length quantum number n is, the more suitable the SOWR can be designed as a single channel high-efficiency energy storage device, and the more convenient and safer the experimental operation will be.

For the EM waves with frequency f_{n1} in types I and II SOWRs, we use numerical results to verify (14) and Table 3. $x_{\max,U1}$ and $x_{\max,L1}$ can be calculated by (5). In Fig. 5, we plot the results of the upper and lower arms of types I and II SOWRs. Making use of (14) and Table 3, we also draw the fitting curves of $x_{\max,U1}$ and $x_{\max,L1}$ in Fig. 5. From Fig. 5 one can see that all of the points are on the fitting curves. It means that the numerical results are accordant with fitting formula very well.

ii) In types I and II SOWRs, for the EM waves with photonic frequency f_{n2}, more than one maximal photonic localization sites are generated in both upper and lower arms. In type III SOWRs, for the EM waves with photonic frequencies f_{n1} and f_{n2} more than one maximal photonic localization sites are generated in both upper and lower arms. Additionally, we find that in a SOWR the distance between two adjacent sites of maximal photonic localization is invariant and the constants in upper and lower arms are all the same. We express this constant as $\triangle x_{\max}$, then the distance from the qth site of the maximal photonic localization to node 1 is

$$x_{\max,\nu q} = x_{\max,\nu 1} + (q - 1)\triangle x_{\max}. \tag{15}$$

In addition, we obtain the fitting formulae of $x_{\max,\nu 1}$ ($\nu = $ U, L) and $\triangle x_{\max}$ as follows:

$$W_g = C_{7g}n^{C_{8g}} + C_{9g} \tag{16}$$

where, $g = 1, 2, 3$, $W_1 = x_{\max,U1}$, $W_2 = x_{\max,D1}$, and $W_3 = \triangle x_{\max}$. The values of coefficients $C_{ig}(i = 7, 8, 9; \ g = 1, 2, 3)$ in (16) are shown in Table 4.

TABLE 4

Values of coefficients in (16) for EM waves with frequency f_{n1} and f_{n2}

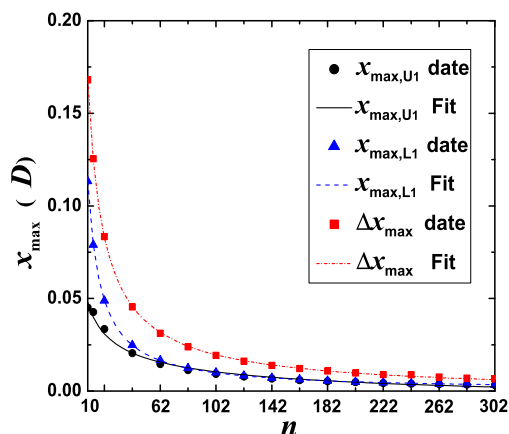| Category	C_{71}	C_{81}	C_{91}	C_{72}	C_{82}	C_{92}	C_{73}	C_{83}	C_{93}
Type I- f_{n2}	1.324	−1.643	0.002509	0.1293	−0.7303	−0.001821	0.9392	−1.248	0.002201
Type II- f_{n2}	3.552	−1.590	0.002053	0.2375	−0.7616	−0.001726	2.0570	−1.222	0.002005
Type III- f_{n1}	4.985	−1.451	0.003304	0.5694	−0.8376	−0.001827	3.506	−1.159	0.002739
Type III- f_{n2}	0.1601	−0.4091	−0.01163	1.325	−1.071	0.0004986	1.318	−0.8872	−0.002133

Fig. 6. W_g versus n in type III SOWRs for the EM waves with frequency f_{n2}. The black spots, blue triangles, and red squares represent the numerical results of $x_{max,U1}$, $x_{max,L1}$, and $\triangle x_{max}$, respectively. The black solid line, blue dash line, and red dot line represent the results of fitting formulae of $x_{max,U1}$, $x_{max,L1}$, and $\triangle x_{max}$ with n for (16), respectively.

From (16) and Table 4, one can see that W_g ($g = 1, 2, 3$) is a monotonous decreasing power function of n, which asymptote is $W_g = C_{9g} \approx 0$. It means that with the increment of n, the position of the first site of maximal photonic localization tends to node 1 gradually in both upper and lower arms, and meanwhile the distance between two adjacent sites of maximal photonic localizations also tends to be smaller and smaller. The reason is as follows: with the increment of n, the site number of the maximal photonic localization increases gradually in both upper and lower arms. Therefore, for experimental convenience and safety, the smaller the loop length quantum number is, the safer the SOWRs with more than one site of maximal photonic localization are for designing multi-channel high efficiency energy storage devices, and then, the more convenient the operation will be.

As an example, we use type III SOWRs to verify the fitting formula (16) and Table 4 for the EM waves of frequency f_{n2}. From (2), one can obtain $m : n = (2j − 1) : [2(2j + 1)]$ for type III SOWRs, where $j \geq 2$. $x_{max,U1}$, $x_{max,L1}$ and $\triangle x_{max}$ can be calculated by (5). In Fig. 6, we plot the results of the upper and lower arms of types III SOWRs. Making use of (16) and Table 4, we also draw the fitting curves of $x_{max,U1}$, $x_{max,L1}$, and $\triangle x_{max}$ in Fig. 6. From Fig. 6, one can see that all of the points are on the fitting curves. It means that the numerical results are accordant with fitting formula very well.

4. Conclusion

Based on our recent work [28], by referencing the single-electronic-mesoscopic ring being able to generate a huge electronic persistent current, we design three types of SOWRs being capable of producing strong photonic localizations and study the features of l_{max}, N, and x_{max}.

First, we investigate l_{max} and find that l_{max} increases as a quadratic function with the increment of n. The fitting formula is obtained. This feature possesses important potential applications for designing such as high efficiency energy storage devices, optical switches, high power super luminescent light emitting diodes, and so on.

Second, we research N and obtain the following properties. i) In type I SOWRs, for the EM waves with frequency f_{n1} there only exists one site of maximal photonic localization in both upper and lower arms. For the EM waves with frequency f_{n2} there exist more than one sites of maximal photonic localizations in both upper and lower arms. The site number increases linearly with the increment of n and the growth rate is 1. ii) In type II SOWRs, for the EM waves with frequency f_{n1} there only exists one site of maximal photonic localization in both upper and lower arms. For the EM waves with frequency f_{n2} there exist more than one sites of maximal photonic localizations in both upper and lower arms. The site number increases linearly with the increment of n and the growth rate is 1/2. iii) In type III SOWRs, for the EM waves with frequency f_{n1} or f_{n2} there only exists one site of maximal photonic localization in both upper and lower arms. For the EM waves with frequency f_{n2}, there exist more than one sites of maximal photonic localizations in both upper and lower arms. The site number increases linearly with the increment of n and the growth rate is 1/4. The properties of single-site (multi-sites) of maximal photonic localizations in SOWR possess potential applications in producing single- (multi-) channel high efficiency energy storage devices.

Finally, we study x_{max} and obtain the following features. i) When only one site of maximal photonic localization is generated in both upper and lower arms, we find that with the increment of n, the position of this site tends to the midpoint of the upper and lower arms, respectively. Therefore, the larger the n is, the more suitable the SOWRs are for designing single channel high efficiency energy storage devices, and the more convenient and safer the operation will be. ii) When mre than one sites of maximal photonic localizations are produced in both upper and lower arms, we find that the distance between two adjacent sites of maximal photonic localization is invariant and the constants in upper and lower arms are all the same. We obtain the formula of $x_{max,q}$. It is helpful to decide the connection positions of multi-channel energy storage devices.

In conclusion, this approach of referencing the single-electronic-mesoscopic ring to design the SOWR may offer a new way for devising optical structures being capable of generating strong photonic localizations, and may also deepen people's knowledge on the correlation between OWN and electronic mesoscopic network. Our designed SOWRs may possess potential applications for designing single- (multi-) channel high-efficiency energy storage devices, optical switches, high power super luminescent light emitting diodes, and so on.

References

[1] E. Yablonovitch, "Inhibited spontaneous emission in solid-state physics and electronics," *Phys. Rev. Lett.*, vol. 58, no. 20, pp. 2059–2062, May 1987.

[2] S. John, "Strong localization of photons in certain disordered dielectric superlattices," *Phys. Rev. Lett.*, vol. 58, no. 23, pp. 2486–2489, Jun. 1987.

[3] S.-Y. Lin, E. Chow, V. Hietala, P. R. Villeneuve, and J. D. Joannopoulos, "Experimental demonstration of guiding and bending of electromagnetic waves in a photonic crystal," *Science*, vol. 282, no. 5387, pp. 274–276, Oct. 1998.

[4] S. Noda, K. Tomoda, N. Yamamoto, and A. Chutinan, "Full three-dimensional photonic bandgap crystals at near-infrared wavelengths," *Science*, vol. 289, no. 5479, pp. 604–606, Jul. 2000.

[5] S. Ogawa, M. Imada, S. Yoshimoto, M. Okano, and S. Noda, "Control of light emission by 3D photonic crystals," *Science*, vol. 305, no. 5681, pp. 227–229, Jul. 2004.

[6] Z. Yu, Z. Wang, and S. Fan, "One-way total reflection with one-dimensional magneto-optical photonic crystals," *Appl. Phys. Lett.*, vol. 90, no. 12, pp. 121133-1–121133-3, Mar. 2007.

[7] K. A. Atlasov *et al.*, "1D photonic band formation and photon localization in finite-size photonic-crystal waveguides," *Opt. Exp.*, vol. 18, no. 1, pp. 117–122, Jan. 2010.

[8] S. R. Huisman, R. V. Nair, L. A. Woldering, M. D. Leistikow, A. P. Mosk, and W. L. Vos, "Signature of a three-dimensional photonic band gap observed on silicon inverse woodpile photonic crystals," *Phys. Rev. B*, vol. 83, no. 20, pp. 205313-1–205313-7, May 2011.

[9] P. Sun and J. D. Williams, "Metallic spiral three-dimensional photonic crystal with a full band gap at optical communication wavelengths," *IEEE Photon. J.*, vol. 4, no. 4, pp. 1155–1162, Aug. 2012.

[10] Y. H. Cheng, C. W. Tsao, C. H. Chen, and W. J. Hsueh, "Strong localization of photonics in symmetric Fibonacci superlattices," *J. Phys. D, Appl. Phys.*, vol. 48, no. 29, pp. 295101-1–295101-8, Jun. 2015.

[11] H. Wang, X. Wu, and D. Shen, "Localized optical manipulation in optical ring resonators," *Opt. Exp.*, vol. 23, no. 21, pp. 27650–27660, Oct. 2015.

[12] L. Dobrzynski, A. Akjouj, B. Djafari-Rouhani, J. O. Vasseur, and J. Zemmouri, "Giant gaps in photonic band structures," *Phys. Rev. B*, vol. 57, no. 16, pp. R9388–R9391, Apr. 1998.

[13] Z. Q. Zhang *et al.*, "Observation of localized electromagnetic waves in three-dimensional networks of waveguides," *Phys. Rev. Lett.*, vol. 81, no. 25, pp. 5540–5543, Dec. 1998.

[14] S.-K. Cheung, T.-L. Chan, Z.-Q. Zhang, and C. T. Chan, "Large photonic band gaps in certain periodic and quasiperiodic networks in two and three dimensions," *Phys. Rev. B*, vol. 70, no. 12, pp. 125104-1–125104-7, Sep. 2004.

[15] Z.-Y. Wang and X. Yang, "Strong attenuation within the photonic band gaps of multiconnected networks," *Phys. Rev. B*, vol. 76, no. 23, pp. 235104-1–235104-7, Dec. 2007.

[16] C. Caer, X. L. Roux, and E. Cassan, "Enhanced localization of light in slow wave slot photonic crystal waveguides," *Opt. Lett.*, vol. 37, no. 17, pp. 3660–3662, Sep. 2012.

[17] L. Zhang *et al.*, "A high-speed second-order photonic differentiator based on two-stage silicon self-coupled optical waveguide," *IEEE Photon. J.*, vol. 6, no. 2, Apr. 2014, Art. no. 7900505.

[18] X. Xu, X. Yang, S. Wang, T. C. Liu, and D. Deng, "Sufficient condition for producing photonic band gaps in one-dimensional optical waveguide networks," *Opt. Exp.*, vol. 23, no. 21. pp. 27576–27588, Oct. 2015.

[19] C. W. Tsao, Y. H. Cheng, and W. J. Hsueh, "High-order micro-ring resonator with perfect transmission using symmetrical Fibonacci structures," *Opt. Lett.*, vol. 40, no. 18. pp. 4237–4240, Sep. 2015.

[20] J.-X. Hu and Y.-T. Fang, "Self-trapped band and semi-opening movable cavity," *IEEE J. Quantum Electron.*, vol. 52, no. 7, Jul. 2016, Art. no. 6400407.

[21] Y. Su, F. Liu, Q. Li, Z. Zhang, and M. Qiu, "System performance of slow-light buffering and storage in silicon nano-waveguide," *Proc. SPIE*, vol. 6783, Oct. 2007, Art. no. 6783.

[22] T. S. Kao, S. D. Jenkins, J. Ruostekoski, and N. I. ZheludevKao, "Coherent control of nanoscale light localization in metamaterial: creating and positioning isolated subwavelength energy hot spots," *Phys. Rev. Lett.*, vol. 106, no. 8, pp. 085501-1–085501-4, Feb. 2011.

[23] M. Aghaie, D. Hebri, A. Ghaedzadeh, and H. Bazyar, "Controlled bistability by using array defect layers in one-dimensional nonlinear photonic crystals," *Appl. Opt.*, vol. 51, no. 13, pp. 2477–2484, May 2012.

[24] Z. Zang *et al.*, "High-power (> 110 mW) superluminescent diodes by using active multimode interferometer," *IEEE Photon. Technol. Lett.*, vol. 22, no. 10, pp. 721–723, May 2010.

[25] Z. Zang, K. Mukai, P. Navaretti, M. Duelk, C. Velez, and K. Hamamoto, "Thermal resistance reduction in high power superluminescent diodes by using active multi-mode interferometer," *Appl. Phys. Lett.*, vol. 100, no. 3, pp. 031108-1–031108-4, Jan. 2012.

[26] S. Sengupta and A. Chakrabarti, "Wave propagation in a quasi-periodic waveguide network," *Physica E*, vol. 28, no. 1, pp. 28–36, Jan. 2005.

[27] Z. Tang, X. Yang, J. Lu, and C. T. Liu, "Super-strong photonic localization in symmetric two-segment-connected triangular defect waveguide networks," *Opt. Commun.*, vol. 331, pp. 53–58, 2014.

[28] S. Xiao, X. Yang, L. Cai, and T. C. Liu, "Giant persistent current in an open mesoscopic ring," *Eur. Phys. J. B*, vol. 86, no. 3, pp. 1–6, Mar. 2013.

[29] Y. Imry, *Introduction to Mesoscopic Physics*. New York, NY, USA: Oxford Univ. Press, 2002.

[30] J. B. Xia, "Quantum waveguide theory for mesoscopic structures," *Phys. Rev. B*, vol. 45, no. 7, pp. 3593–3599, Feb. 1992.

[31] Z. Q. Zhang and P. Sheng, "Wave localization in random networks," *Phys. Rev. B*, vol. 49, no. 1, pp. 83–89, Jan. 1994.

[32] Y. Liu, Z. Hou, P. M. Hui, and W. Sritrakool, "Electronic transport properties of Sierpinski lattices," *Phys. Rev. B*, vol. 60, no. 19, pp. 13444–13452, Nov. 1999.

[33] A. M. Jayannavar and P. Singha Deo, "Persistent currents in the presence of a transport current," *Phys. Rev. B*, vol. 51, no. 15, pp. 10175–10178, Apr. 1995.